Sohrabi *et al. Chem. Biol. Technol. Agric. (2022) 9:82*
https://doi.org/10.1186/s40538-022-00352-w

Chemical and Biological Technologies in Agriculture

RESEARCH

Open Access

# Plant-based nano-fertilizer prepared from *Paulownia Tomentosa*: fabrication, characterization, and application on *Ocimum basilicum*

Yousef Sohrabi[1*], Firouzeh Sharifi Kalyani[1], Moslem Heydari[2], Majed Yazdani[3], Khalid M. Omer[4] and Ali Reza Yousefi[2]

## Abstract

**Background:** The use of hazardous and toxic chemical material has become limited by the green synthesis of nanoparticles (NPs) from plants and other living organisms. In the current study, a new nano-fertilizer was green synthesized from *Paulownia tomentosa* leaves and then its effectiveness in alleviation of drought stress in *Ocimum basilicum* was investigated. Five concentrations of nano-fertilizer (0, 50, 70, 90 and 110 ppm) at three irrigation regimes including 100% of field capacity (IRF100), 75% of field capacity (IRF75), and 50% of field capacity (IRF50) were evaluated. Nano-fertilizers were prepared using the green hydrothermal method.

**Results:** Based on TEM analyses nanoparticles sizes were 5–8 nm. The results of FTIR appearance indicated the main distinctive peaks of the Paulownia-based nano-fertilizer (NFPs) in the spectrum. In addition, the nitrogen peaks in the XPS spectra indicate that the prepared carbon dots NFPs are nitrogen-doped. Moreover, there are functional groups, such as COOH or OH groups on the surface of Paulownia-based nano-fertilizer (NFPs). The results illustrated that drought stress increased proline (73%), alcohol-soluble carbohydrates (78%), and malondialdehyde (41%) in comparison with normal irrigation; in contrast, soluble proteins (73%), Chlorophyll a (46%), Chlorophyll b (39%), Chlorophyll total (42%), and carotenoid (77%) were reduced in the same condition. The *O. basilicum* biological yield was reduced in moderate (12.40%) and severe (24.42%) drought stress in comparison with full irrigation conditions (IRF100). Paulownia-based nano-fertilizer (NFPs) caused an increase in soluble proteins and photosynthetic pigments. Application of NFP-90 reduced the production of proline and malondialdehyde, respectively, 51.8% and 30.8% compared to non-application under severe stress conditions, which indicates alleviated the adverse effect of drought stress. The highest biological yield of basil was obtained at a 110 ppm concentration of NFPs.

**Conclusion:** Overall, results showed that using NPs biosynthesized from Paulownia leaves could be an economically and environmentally friendly method as a nano-fertilizer.

*Correspondence: y.sohrabi@uok.ac.ir

[1] Department of Agronomy and Plant Breeding, University of Kurdistan, Sanandaj, Iran
Full list of author information is available at the end of the article

**Highlights**

- Plant-based nano-fertilizer prepared from Paulownia.
- Nano-fertilizer prepared from Paulownia characterized by TEM, XPS, XRD, and FTIR.
- Use of Nano-fertilizer prepared from Paulownia (NFPs) had a significant effect on O. basilicum.
- The highest basil biological yield was obtained at NFP-110.

**Keywords:** Basil, Green synthesized, Paulownia, MDA, NPs, XPS

**Graphical Abstract**

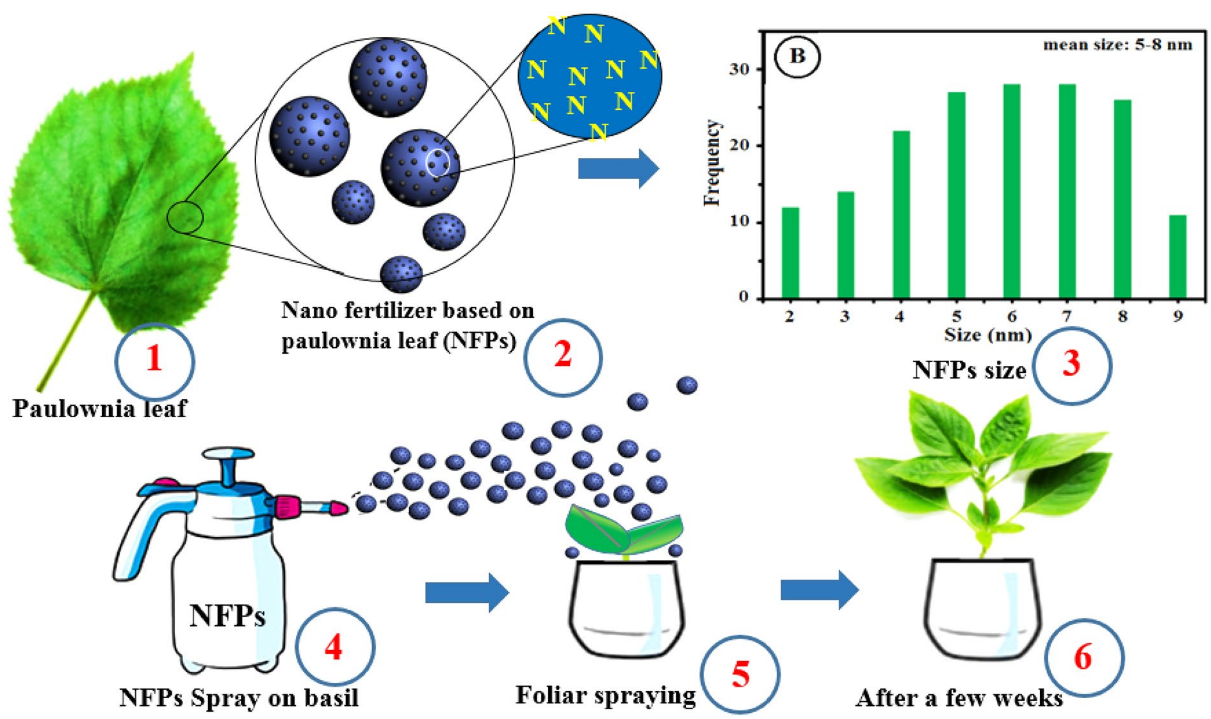


## Introduction

Feeding the growing world population, which is projected to reach 9 billion by 2050 is the most important challenge facing agriculture. Conventional agriculture or organic farming practices cannot meet the growing demand for food [1]. The use of different fertilizers in the agriculture field is inevitable for enhancing and increasing crops. However, the adverse effects of agro-chemical have faced the environment and agriculture with major challenges [1]. For example, the high consumption of nitrogen fertilizers, has caused problems, such as surface water and groundwater resources contamination due to nitrate leaching [1]. In addition, the excessive use of fertilizers not only imposes additional costs on the farmers, but is also considered to be a barrier to sustainable agriculture development and causes food elements imbalance, food chain disturbances, and various environmental problems [2]. Various solutions have been proposed to solve these problems, including the use of nanotech. The use of elements at the nanoscale not only increases the efficiency of nutrients for the plant but also reduces the use of fertilizers due to the high surface-to-volume ratio [3–5].

Nanotechnology plays an important role in producing agricultural products [6]. The NPs have high reactivity levels because of specific surface area and due to their small size and high surface/volume ratio. Because of the unique properties of nanotech, their use in agriculture has been very popular in recent years [3–5]. Nanotech-based agrochemical can influence the absorption and maintenance of nutrients and the physical and chemical properties of the soil. In addition, these particles have a high ability to absorb heavy metals and organic matter from the soil [7, 8]. For synthesizing NPs several different methods have been introduced [9, 10]. Because of high energy consumption and non-degradable toxic agents, their use is limited in bio-systems [9]. Therefore, nanoparticle synthesis was shifted toward eco-friendly methods, such as the green synthesis approach. Green synthesis of NPs is achieved using important three sources, such as autotrophs (plant and algae) [11], bacteria, and fungi [12, 13]. Due to easy availability and simplicity, plant-mediated nanoparticles synthesis is gaining significant momentum in interdisciplinary fields. There are abundant phytoconstituents that act as stabilizing, reducing, and capping compounds during NPs synthesis [12, 14]. One of the ways to NPs green synthesis is by mixing metal salts solution with the extract of plant parts [14]. Different plant parts are utilized in green synthesis including; leaf, root, flower, seeds, and, fruit [15].

The *Paulownia Tomentosa* an ornamental tree, with low-demand water and fast-growing are native to China and East Asia which includes nine species [16]. In addition, there are bred in North America, Australia, Europe, and Japan [17]. Paulownia's characteristics of rot resistance, dimensional stability, and a very high ignition point ensure the popularity of this timber in the world market [18, 19]. This species has value for its small sawn timbers that are in demand for specialty products. It is also used to treat various diseases in China [20].

The adverse effects of taking chemical drugs have increased the tendency toward the production, utilization, and processing of plants that have medicinal properties. In recent years, the use of medicinal plants has taken much attention [21]. The basil (*Ocimum basilicum* L.) is an annual plant of the Lamiaceae family with rich medicinal properties which the seed can easily reproduce [22]. The *O. basilicum* has antioxidant, antimicrobial, and analgesic properties, and is used in traditional medicine to treat diseases, such as diabetes, fever, liver disease, gastric ulcer, cardiovascular disease, digestive disorders, arthritis, Nyctalopia, blood lipids, and Dyspnea [23, 24]. Basil contains sesquiterpenoids, monoterpenes, and flavonoids [21, 25]. The content of basil's secondary metabolites content is affected by environmental factors and applied management practices. Environmental stress (biotic and abiotic), limits the production and yield of crops and also affects the content of secondary metabolites and other compounds in plants [26, 27].

Drought stress is the most important abiotic stress that decreases plants' growth, yield, and production of plants [28]. In recent decade temperature rise and changes in rainfall patterns have increased the effects of drought stress on agriculture in many parts of the world [29]. Understanding the response of plants to water deficit can be very helpful in finding suitable solutions to improve plant tolerance to drought stress [30]. The aim of this study is the investigate the possible effects of NFPs on the physiology characteristics of *O. basilicum* under different irrigation regimes.

## Materials and methods

### Materials

Metal salts (nitrate and chloride sources) were purchased from Merck chemical Co. Sigma-Aldrich Co provided Quinine sulfate (Quinine hemisulfate salt monohydrate) and HCl. The chemicals used throughout this work were of analytical grade and were used as received. In addition, doubly distilled, deionized Millipore water was utilized.

### Fabrication of NFs prepared from Paulownia powder (NFP)

*Paulownia tomentosa* leaves which were planted in the Agriculture College of Sulaymaniyah University, Iraq, was used as a source of Paulownia leaves. The leaves were collected in the fully grown stage (when the leaf nitrogen content was measured at its highest level). The leaves were cleaned and washed with distilled water several times, then dried in the shade for 1 week. Using the grinder, the dried leaves were powdered.

NFPs were composed of carbon nanodots and they were prepared using the green hydrothermal method. In summary, 0.1 g of Paulownia leaves powder was solved with 10 mL distilled water, followed by 0.2 ml HCl (0.5 M) was added to the solution. Then, the solution with a Teflon-cowered was transferred to 185 °C autoclave for 20 h. Afterward, the solution was cooled down to room temperature, followed by filtration, and centrifuged at 12,000 rpm for 30 min. The solution was then mixed with chloroform to purify the NFs leaving the salts and ions in an aqueous layer. The NFs in chloroform solution is then heated slowly on the heater to remove all chloroform. The solid Carbon dots (CDs) were then mixed with water to form CDs dispersed in a water solution.

### Physio-chemical characterization of NFs of Paulownia powder (NFP)

The particle size was measured by the transmission electron microscopy (TEM) model JEOL 2010 F. Fluorescence emission measurements were recorded with a Flurolog-3 fluorescence spectrophotometer (Horiba, USA). UV–Vis absorption spectra were measured by spectrophotometer (Cary 6000, Agilent, USA). To prepare pellets of NFPs, ca. 2 mg of NFPs, 200 mg of spectroscopic grade KBr were combined. A Varian 640 FTIR spectrophotometer (Palo Alto, CA, USA) was used with a resolution of 4 $cm^{-1}$ and 64 scans per sample to record IR spectra (4000–400 $cm^{-1}$). Some bands shielded by the extensive OH bending mode of bound water were elucidated using an FTIR spectrometer (Palo Alto, CA,

**Table 1** Chemical and physical characteristics of the used soil

| Soil texture | Organic C (g $kg^{-1}$) | pH | Sand (%) | Silt (%) | Clay (%) | N (%) | EC (ds $m^{-1}$) | K (ppm) | P (ppm) |
|---|---|---|---|---|---|---|---|---|---|
| Clay sand | 0.76 | 7.8 | 34 | 31 | 35 | 0.52 | 0.96 | 180 | 8.5 |

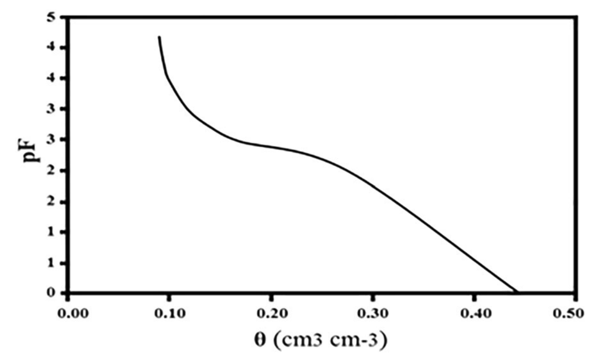


**Fig. 1** Soils moisture content curve

USA) armed with an evacuation line. In this regard, the pellets were created with no KBr. To press NPs (about 4 mg), NFPs specimens in a standard tool, a pressure of 98 kN $cm^{-2}$ was used to create pellets in diameter of 13 mm. High-resolution XPS spectra were recorded by Kratos Analytical using Al Kα radiation as the excitation source. In addition, XRD spectra were recorded by UltimaIV (Rigaku, Japan).

### Planting and applying NFPs on *O. basilicum*

This study was conducted in the research greenhouse of the Agriculture Faculty, Kurdistan University, Iran (35.3219° N, 46.9862° E, 1,538 masl) in 2020. The basil (*Ocimumbasilicum*) seeds "prepared from Agricultural and Natural Resources Research and Education Center of Kurdistan (ANRRECK)" were soaked first with sodium hypochlorite for a few min and washed with water). The soil was sterilized at 121 °C and 1.5 atmospheres for 1 h after air drying (chemical and physical characteristics of soil are shown in Table 1). Then, the 40 seeds of *O. basilicum* were planted in plastic pots (25 × 15 × 25 cm). The pots were then moved to a greenhouse with 26/18 °C temperature, 15/9 h a day/night photoperiod with 60 ± 10% relative humidity and 750 µmol $m^{-2}$ $s^{-1}$ photosynthetic photon flux density. After seedlings emergence and ensuring their complete establishment, the plants were thinned in the 4-leaf stage and kept eight plants per pot. Different concentrations of nano-fertilizers prepared from Paulownia (NFP) including 0, 50, 70, 90, and 110 ppm (respectively, abbreviation: NFP-0, NFP-50, NFP-70, NFP-90, and NFP-110), were applied on *O. basilicum* which were grown at the different irrigation regimes including 100%, 75%, 50% of field capacity (respectively, IRF100, IRF75, and IRF50). The factorial experiments were performed by a completely randomized design (CRD) with three replications.

Spraying of NFPs was performed in two stages, 4 weeks (8-leaf stage) and 7 weeks (10-leaf stage) after emergence. Irrigation treatments (IRF100, IRF75, and IRF50) were applied from 4 weeks after emergence. To apply different irrigation regimes, the pots' soil moisture curve was determined by a pressure plate (Fig. 1).

Then, the water potential of the soil and irrigation time in different irrigation was determined by the weighted method. The pots were weighed each day and after the soil moisture potential of the pots reached the desired treatment level, the pots were irrigated related to that treatment. During the experiment, the irrigation time of the pots varied at different levels of irrigation. Before applying different irrigation treatments, all the pots were irrigated uniformly.

### Data collection on plant traits

To determine and measure basil's physiological traits, before harvesting the plant, mature leaf samples were collected and immediately transferred to the laboratory by the nitrogen tank and placed in the freezer at −40 °C until measuring time. Different physiological traits were measured. Briefly, the proline content was measured by the Bates et al. [31] method [31]. By Bradford's [32] method soluble proteins were recorded [32]. The Anthrone method was used to measure the soluble leaf carbohydrates [33]. After preparing leaf samples and different readings at different wavelengths, Chlorophyll a, b, total, and carotenoid content were calculated using Eqs. 1–4 [34]:

$$Chla = (12.25 \times A\,663) - (2.79 \times A\,646) \quad (1)$$

$$Chlb = (21.21 \times A\,646) - (5.1 \times A\,663) \quad (2)$$

$$Chlt = Chl_a + Ch_b \quad (3)$$

$$Carotenoid = (1000\,A\,470) - (1.82 \times Chl_a) - (85.02 \times Ch_b) / 198 \quad (4)$$

Malondialdehyde is the final product of the lipid peroxidation membrane. Therefore, measurement of

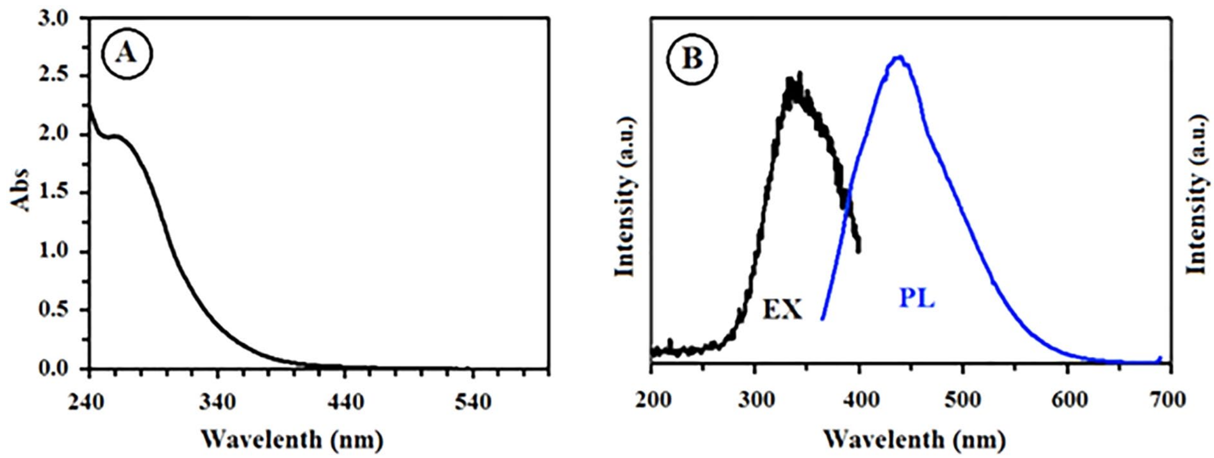


**Fig. 2** Optical properties of NFP. **A** UV–Vis absorption spectrum, **B** excitation (black line), and fluorescence emission (blue line) spectra. For collecting fluorescence emission spectra, the solution excited at 350 nm, for the collecting excitation spectra, the emission wavelength was 450 nm

malondialdehyde in plant's leaves under drought stress seems very necessary. Based on this, the content of *O. basilicum* malondialdehyde leaves was measured by Heath and Packer [35] method (Eq. 5) [35].

$$MDA = ((W\ 532nm/155) / 0.3 - (W\ 600nm/155) / 0.3) \quad (5)$$

The Biological yield was also measured by placing the plants for 48 h in an oven at 75 °C and then weighed via a digital balance with an accuracy of 0.01 g.

### Statistical analysis

The data were analyzed with SAS software (version 9.4) and SPSS (Version 16.0). The means were compared utilizing the least significant difference test (LSD) and analysis of variance (ANOVA) at the significance level of 0.05.

## Result

### Physio-chemical characterization NFPs

UV–Vis absorption spectra and fluorescence spectra were used to investigate the optical properties of the NFs. Figure 2 shows the UV–Vis spectrum peak of about 265 nm (Fig. 2a), and the fluorescence peak ca 445 nm (Fig. 2b). The UV–Vis spectrum shows a typical 265 nm absorption peak that assigns for π to π* transition of C=C bonds in the graphene sheets [36]. The fluorescence emission peak at 445 nm (Fig. 2b, blue emission), when excited at 350 nm. Thus, the NFPs are blue luminescent nanomaterials.

To obtain the size and shape of NFs, transmission electron microscope (TEM) images were used, as shown in Fig. 3a. The nanoparticles were spherical with a size distribution between 5 and 8 nm, as shown in the histogram (Fig. 3b). Crystal structure of the NFP was tested using XRD spectrum (Fig. 3c). XRD spectra show a broad peak at 22–25°, assigning for the amorphous graphitic structure of carbon dots (Fig. 3c). The spectrum showed a broad weak peak centered at about 240. FTIR and XPS spectra were recorded to probe the chemical functional groups on the surface of the NFs. Figure 3d shows the FTIR spectrum of the NFs. Wide broad peaks above 3000 $cm^{-1}$ and one sharp peak at 1600 $cm^{-1}$ were recorded. To further know the chemical functional groups on the surface of carbon dots NFs, high-resolution X-ray photoelectron spectroscopy (HR-XPS) was performed. Broad absorption peak between 2700 and 3600 $cm^{-1}$ is attributed to the stretching mode of O–H, and at 2900 $cm^{-1}$ to the C–H stretching. A small absorption peak at 1630 $cm^{-1}$ assigns for C=C of the graphene [37, 38].

By XPS analysis the survey and resolved spectra of each identified element (Fig. 4). The survey spectra show three major peaks corresponding to O 1 s (~530 eV), C 1 s (~282 eV), and N 1 s (400 eV) (Fig. 4A). Resolved O 1 s spectra display three peaks centered at 529.31, 530.9, and 531.52 eV corresponding to C–O, C=O, and O–H, respectively [39], De convoluted C 1 s spectra (Fig. 4c) show two peaks at 282.9, and 284.5, corresponding to graphitic sp2 C=C, and C–O/C–OH, respectively [40]. The N 1 s spectra (Fig. 4d) show three peaks, at 398.1 eV, which corresponds to C–N–C nitrogen atom, and the second one 399.7.1 eV corresponds to N–H eV, and the last one 400.9 corresponds to C=N [41]. The nitrogen peaks in the XPS spectra indicate that the prepared carbon dots NFPs are nitrogen-doped. Moreover, there are functional groups, such as COOH or OH groups on the surface of NFPs.

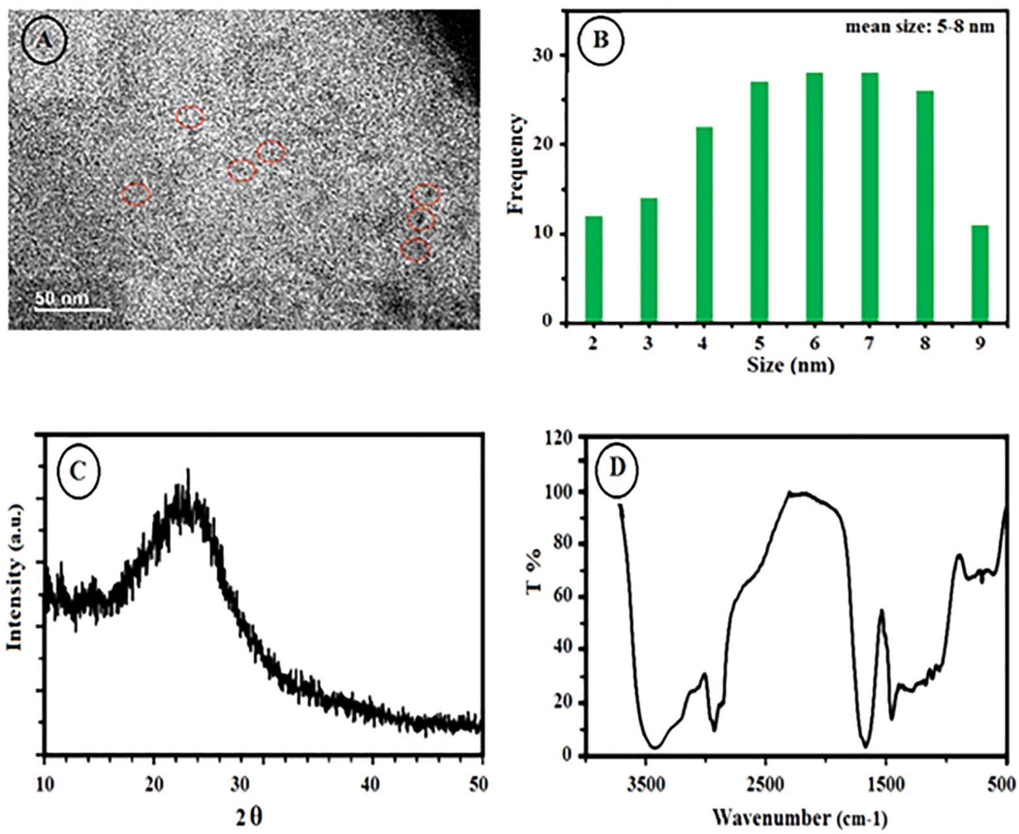


**Fig. 3** TEM of carbon NFP (**A**), histogram of the TEM images (**B**), 250 particles were counted XRD spectrum (**C**), FTIR spectrum (**D**)

#### Effect of treatments on physiological traits of *O. basilicum*

Based on analysis of variance results, the proline contents, soluble proteins, soluble carbohydrates, chlorophyll a, chlorophyll b, total chlorophyll and malonedealdehyde (MDL) of *O. basilicum* significantly affected ($P \leq 0.01$) by application of Paulownia-based nanofertilizers (NFP) (Table 2).

The results illustrated that the maximum amount of leaf proline was obtained in IRF50 (mg $g^{-1}$ FW), and the lowest amount (0.11 mg $g^{-1}$ FW) was observed in IRF100 (Fig. 5A). The application of NFPs reduced the amount of proline in leaves. By increasing the concentration of NFPs the amount of leaf proline also decreased at all irrigation levels (Fig. 5A), so that the lowest content of proline was measured in the NFP-110 and IRF100 (Fig. 5A). The amount of proline produced in IRF75 and IRF100 were in the same statistical group, at the same level of fertilization, which indicates the positive effect of NFPs on reducing the stress adverse effects on the plant. As a result, the plant's need to proline production has decreased. The soluble proteins of *O. basilicum* were affected by NFPs and irrigations levels (Table 2). The results show that the highest amounts of soluble proteins of the leaf were obtained under full irrigation conditions (IRF100) and drought stress (IRF50) reduced the soluble proteins of the leaf (Fig. 5B). The use of NFPs under both IRF100 and IRF50 significantly increased the soluble protein (Fig. 5B).

With the occurrence of drought stress and increasing its severity, the content of proline (Fig. 5A) and soluble carbohydrates (Fig. 5B) increased, and in contrast amount of soluble proteins decreased (Fig. 5B). Drought stress, decreases vegetative growth and changes in plant morphological structures and changes the pathway of synthesis of secondary compounds and metabolites through the formation of secondary oxidative stress [42]. Oxidative stress leads to the production of reactive oxygen species (ROSs). The plant reduces the produced ROSs through antioxidant mechanisms (enzymatic and non-enzymatic) [43, 44]. The accumulation of ROSs causes damage to membrane lipids, nucleic acids, and proteins. Therefore, one of the strategies to deal with the damage caused by ROSs is osmotic regulation and the accumulation of compounds, such as proline amino acids. Osmotic regulation is one of the mechanisms for responding to environmental stresses, including drought stress, which, through the

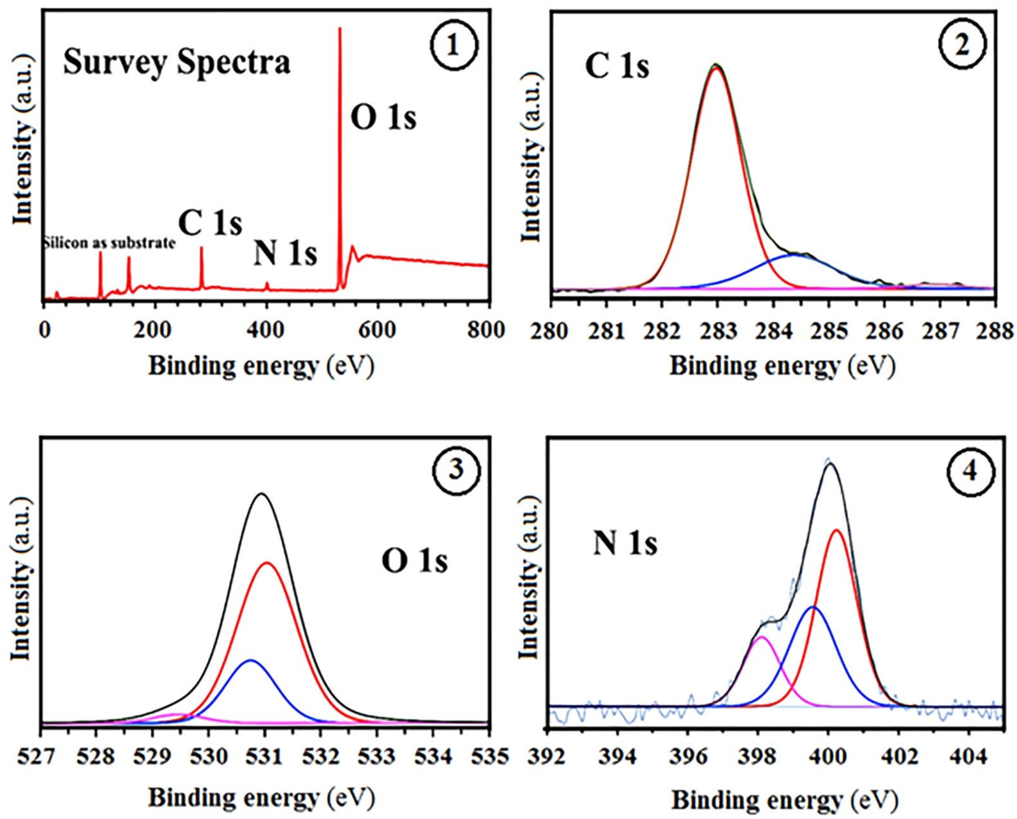


**Fig. 4** High-resolution XPS for NFP, (1) survey spectrum, (2) C 1 s, (3) O 1 s, (4) N 1 s. The NFP were casted on silicon substrate

**Table 2** Analysis of variance of physiological traits of *O. basilicum* as affected by NFPs application under different irrigation regimes

| S.O.V | df | MS | | | | | | | | | |
|---|---|---|---|---|---|---|---|---|---|---|---|
| | | PLN | SP | SCA | SCW | Chl a | Chl b | T Chl | CTD | MDL | BY |
| Irr | 2 | 0.6033** | 44.003** | 1932.8** | 1775.45** | 69.003** | 33.835** | 98.567** | 1.0968** | 0.66748** | 1.541555** |
| NFP | 4 | 0.0658** | 4.750** | 860.73** | 1383.98** | 9.975** | 4.8419** | 27.159** | 0.2199* | 0.10041** | 1.248333** |
| Irr × NFP | 8 | 0.0139*** | 0.63076** | 192.193** | 145.61162 ns | 1.4388** | 1.76421** | 5.75914** | 0.21021* | 0.05414 ** | 0.037666 ns |
| Error | 30 | 0.00283111 | 0.1040289 | 4.974400 | 200.47754 | 0.3389511 | 0.4387178 | 0.9706867 | 0.07154889 | 0.00351333 | 0.03422222 |
| CV | – | 15.14 | 7.81 | 10.15 | 5. 24 | 9.42 | 12.41 | 8.56 | 4. 72 | 4.75 | 8.00 |

* and **, significant at 5 and 1% probability levels, respectively

*PLN* Proline, *SP* Soluble proteins, *SCA* alcohol-soluble carbohydrates, *SCW* water-soluble carbohydrates in, *Chl a* Chlorophyll a, *Chl b* Chlorophyll b, *T Chl* Total chlorophyll, *CTD* Carotenoid, *MDL* Malondialdehyde, and *BY* Biological yield

accumulation of soluble material inside the cells, maintains the cell turgor in the low potentials of the water. In other words, it can be stated that during abiotic stresses such as drought, organic molecules with low molecular weight such as protein, proline, and soluble sugars in the plant organs accumulate to perform osmotic regulation [45]. Amino acids such as alanine, valine, threonine, glycine, serine, and proline are osmotic protectors [46, 47]. In drought stress, the proline amino acid acts as an osmotic regulator and cell protector. The osmotic adjustment process helps the plant grow under water-shortage conditions and allows it to keep its stomata open during stress for a longer time [22]. Proline amino acid is a non-enzymatic antioxidant that by giving electrons to ROSs and stabilizing them, reduces the damage caused by them [22, 43, 48]. Hatami et al. [46] reported that increasing proline amount and reducing soluble proteins in drought stress might be due to decreased protein levels or increased proteolytic activity, which leads to an increase in the total nitrogen content and allows the plant

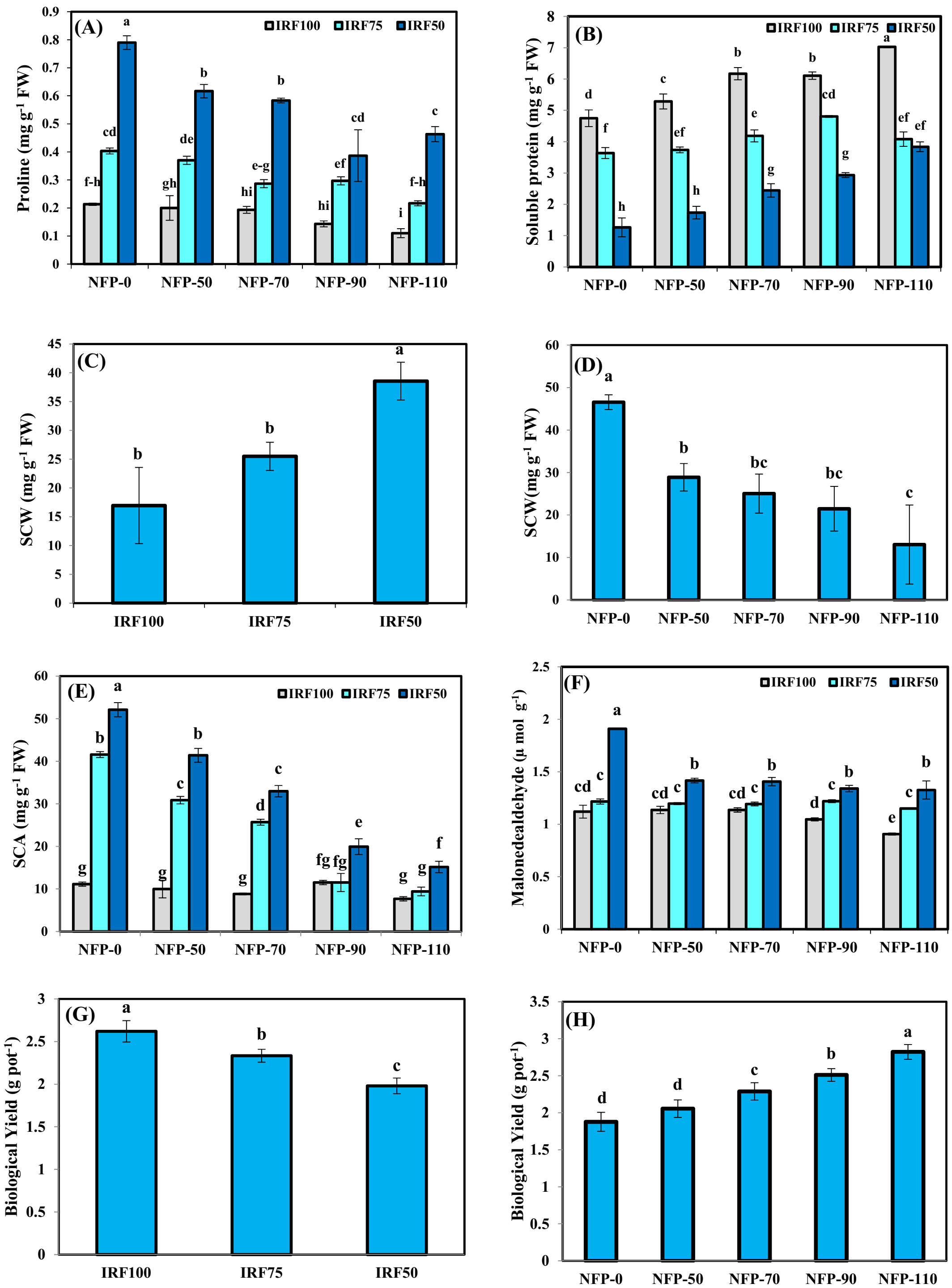


**Fig. 5** Effect of NFPs and different levels of irrigation regimes on proline (**A**), soluble proteins (**B**), water-soluble carbohydrates (**C**, **D**), alcohol-soluble carbohydrates in (**E**), Malonedealdehyde (**F**), Biological Yield (**G**, **H**) of *O. basilicum*. *The vertical bars represent the standard error. (The columns' letters indicate the differences between the different treatments ($p < 0.05$) using the LSD test)

for improving tolerate stress by osmotic adjustment [49]. Other studies have also reported increasing the proline amount in the plant. The results showed that the NFPs reduced leaf proline content, and by increasing the concentration of NFPs, the proline decreased at all irrigation levels. On the other hand, the use of NFPs in both IRF100 and IRF50 conditions significantly increased the soluble protein (Fig. 5).

The results showed that drought stress increased water-soluble carbohydrates, so that the highest water-soluble carbohydrate (39 mg $g^{-1}$) belonged to pots with IRF50 (Fig. 5C). The use of NFPs significantly reduced water-soluble carbohydrates (Fig. 5D). Figure 5d shows that there was no significant difference between NFP-70 and NFP-90. NFP-100 showed the lowest amount of water-soluble carbohydrates (Fig. 5D). The soluble carbohydrates are osmotic regulators. The results indicated that the content of soluble carbohydrates was increased in drought stress conditions (Fig. 5C). Increased soluble carbohydrates can enhance the ability of the plant cell to absorb water in the plant under stress conditions [50, 51]. In addition, soluble sugars, as osmotic regulators, stabilize cell membranes and preserve the cell turgor. A better osmotic regulation occurs in plants that soluble sugars accumulate in response to drought stress [50]. Increasing the amount of soluble sugars such as glucose, fructose, and sucrose in plants under drought stress has been shown in studies by Zandalinas et al. [52]. The highest amount of alcohol-soluble carbohydrates was observed in IRF50 (52.11 mg $g^{-1}$) and IRF75 (41.57 mg $g^{-1}$), respectively (Fig. 5E). This superiority was also observed for plants under severe drought stress (IRF50) in fertilization with NFP-90 and NFP-110 (Fig. 5E).

Different levels of irrigation, different levels of NFPs, and also the interaction of two factors significantly affected ($P < 0.01$) the malondialdehyde (MDL) content of leaf (Table 2). The MDL levels are the indicator for indicating lipid peroxidation of the membrane. However, at all levels of NFPs application, the highest amount of MDL was obtained in IRF50 (Fig. 5F). In IRF50, the highest level of MDL belonged to the control (NFP-0). The application of NFPs significantly reduced MDL. One of the first structures damaged of plant cells is cell membrane lipids in drought stress. Because drought stress, such as other stresses, causes oxidative stress in plant cells and the ROSs produced damage the cell membrane by the membrane lipid peroxidation [53]. MDL is the ultimate product of membrane lipids peroxidation, and its high levels indicate a high level of damage to cell membranes due to stress. Low levels of MDL indicate the plant's resistance to stress [54].

In this study, drought stress and increasing its severity significantly reduced the biological yield (Fig. 5G, H). Increasing damage to cell membranes, degradation of chlorophyll pigments, reducing the synthesis of them under drought stress, and the consequence of this which lead to disruption of cell and cellular organelles activity, reduced assimilation, photosynthesis, and energy production of the plant can be reasons for the decrease of *O. basilicum* biological yield. Reduced growth and yield under limited irrigation conditions have been reported in various plants [21–24]. Damalas [22], Reported that the highest yield of *O. basilicum* was obtained under non-stress conditions and drought stress reduced plant yield [22].

Also, the photosynthetic pigments were affected by different irrigation regimes, various amounts of NFPs, and interaction between these treatments (Table 2). The mean comparison results showed that the highest chlorophyll a, b, total, and carotenoid were obtained under full irrigation conditions and drought stress significantly reduced the chlorophyll content of leaf (Fig. 6). In this study, photosynthetic pigments of the *O. basilicum* such as chlorophylls a, b, total, and carotenoids were reduced under drought stress (Fig. 6). Photosynthetic pigments are sensitive to reducing available water. Damalas [22] reported that drought stress reduced the content of chlorophylls a and b of *O. basilicum* and *M. longifolia*, respectively [22]. In another study, chlorophyll content decreased in *T. vulgaris* under drought stress [55]. Reducing the content of chlorophyll may be due to the imbalance of proteins and increased activity of chlorophyll-degrading enzymes, or may result from damage to the chloroplast due to the production and increase of ROSs [42, 56]. By increasing the amount of NFPs from 90 to 110 ppm, carotenoid increased significantly in plants under stress than full irrigation (Table 2, Fig. 6).

Figure 7 shows the loading plots of principal components 1 and 2 based on the analysis of physiological parameters of *O. basilicum*. Principal component 1 (PC1) captured 77.7% and PC2 11.5% (Fig. 7). Therefore, the cumulative percentage of PC1 and PC2 was 89.2%. Physiological parameters such as Chl a, Chl b, total Chl, soluble proteins contents, and biological yield were under the same group (Fig. 7). In addition, MDL, proline, alcohol soluble carbohydrates, and water-soluble carbohydrates contents, were under the same group. The carotenoid was placed in a separate group. Therefore, a positive correlation has been found between Chl a, Chl b, total Chl, and soluble proteins contents with biological yield. In addition, a positive correlation has been found between MDL, proline, alcohol-soluble carbohydrates, and water-soluble carbohydrates contents, which has a negative correlation with Chl a, Chl b, total Chl and soluble proteins contents, and biological yield parameters. The results showed that the membrane lipid peroxidation reduced

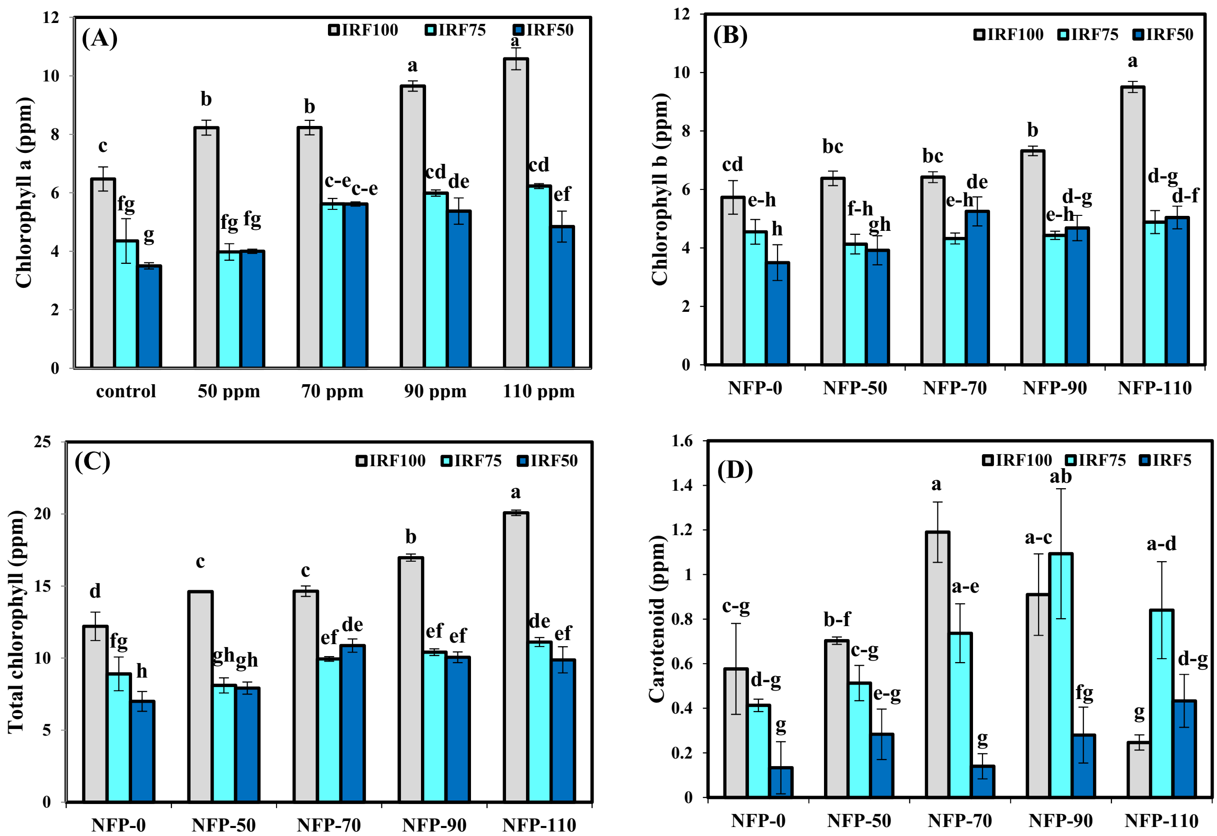


**Fig. 6** Effect of NFPs and different levels of irrigation regimes on Chlorophyll a (**A**), Chlorophyll b (**B**), Total chlorophyll (**C**), and Carotenoid (**D**) of *O. basilicum*. *The vertical bars represent the standard error. (The columns' letters indicate the differences between the different treatments ($p < 0.05$) using the LSD test)

chlorophyll content and biological yield and increasing the MDA increased the production of proline, alcohol soluble carbohydrates, and water-soluble carbohydrates.

This effect of NFPs can be due to increased synthesis of soluble proteins and reduction of their decomposition due to the reduction of proteolytic activity. However, the effect of NFPs on protein content has been varied in different plants and doses [57–59]. In some cases, nanomaterials can create oxidative stress and produce ROSs due to toxicity. This may affect the structure of cells and the primary metabolites, such as protein, carbohydrates, lipids, and secondary metabolites. The protein content decreased due to the application of nano-fertilizers on *H. Vulgare* under drought stress conditions [57, 58]. The use of NFPs significantly reduced the membrane lipid peroxidation in drought stress conditions (Fig. 6) and consequently reduced the adverse effects of stress. In another study, the effect of nano-carbon compounds' concentration was studied on physiological and biochemical characteristics of Henbane (*H. niger* L.) in drought stress conditions. The results showed that the use of NFPs reduced the damage caused by drought stress. In fact, the use of nano-carbon compounds may reduce oxidative stress by increasing the production of protective compounds and enzymatic and non-enzymatic antioxidants. Ghorbanpour and Hatami (2015) reported that using carbon nanoparticles improves antioxidant activity, which results in antioxidant defense from cells and proteins, enzymes, RNA, and DNA against the ROSs and, finally, reduces the effects of drought stress on the plant [60].

Based on the findings of this study, the application of nano-fertilizer increased the content of chlorophyll and carotenoids in *O. basilicum* and significantly reduced the malondialdehyde under drought stress conditions. Aghdam et al. [61] reported that nanoparticles in increased the content of photosynthetic pigments and plant yield of *L. Usitatissimum,* and reduced the amount of hydrogen peroxide and MDL under drought stress which was consistent with the results of our study [61]. In other studies, the use of nano-fertilizers increased the amount of chlorophyll, photosynthesis, and eventually increased growth under stress conditions [62]. In addition, the results of this study showed that the use of nano-fertilizer caused a significant decrease in water-soluble carbohydrates

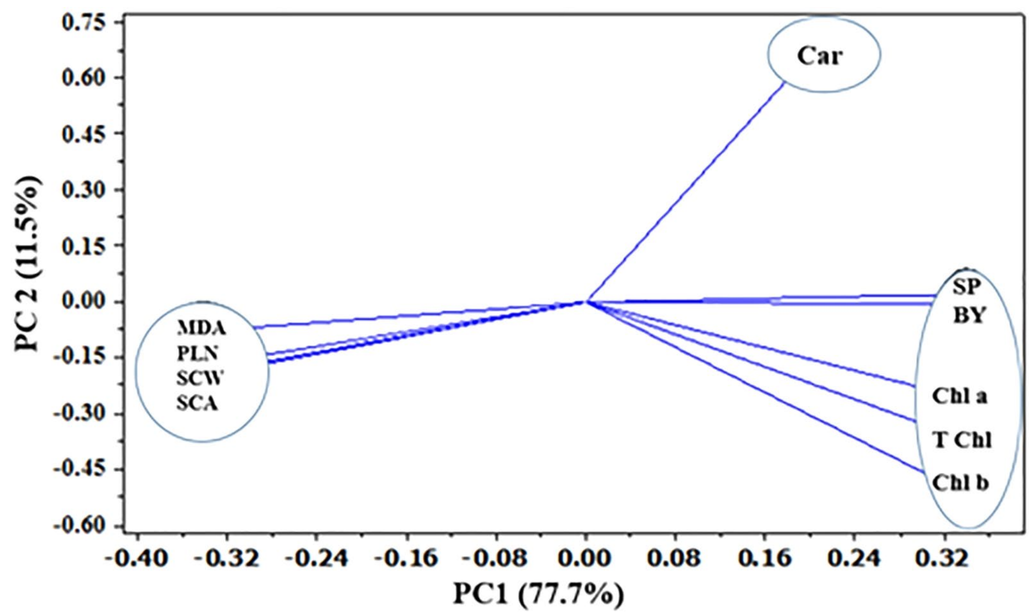


**Fig. 7** Scatter plot of the PC1/PC2 plane shows the relationships between the physiological traits. malondialdehyde (MDA), proline (PLN), alcohol soluble carbohydrates (SCA), water-soluble carbohydrates (SCW), chlorophyll a (Chla), chlorophyll b (Chlb), total chlorophyll (TChl), soluble proteins (SP), and biological yield (BY)

(Fig. 6). In addition, the application of NFPs and increasing their concentration significantly reduced the amounts of alcohol-soluble carbohydrates in plants under drought stress (Fig. 6). Reducing the amount of soluble carbohydrates in the plant due to the use of NFPs under drought stress conditions can be attributed to the role of NFPs in providing the nutrients needed by the plant and improving the synthesis of soluble proteins. The soluble proteins play an important role in increasing the absorption of water due to osmotic adjustments, maintaining the structure of cell membranes, cellular organs, and maintaining the structure of important macromolecules in plant life [45]. These effects of NFPs improved the status of plants, increased the synthesis of photosynthetic pigments, and reduced the need to produce water and alcohol soluble carbohydrates as well as the production and accumulation of proline. However, an increase in the production of enzymatic and non-enzymatic antioxidants resulting from the NFPs application may also be involved in improving the plant condition and reducing the degradation of photosynthetic pigments.

As a result of the current study, the application of nano-fertilizers and increasing their concentration significantly increased the biological yield of *O. basilicum* (Fig. 7). Nano-fertilizers are likely to reduce the damage to photosynthetic pigments or cell organelles such as chloroplast and mitochondria (which contribute to the production of energy) by supplying the nutrients needed to synthesize proteins and antioxidant compounds that play a protective role. On the other hand, increasing the amount of photosynthetic pigments also improves the photosynthesis and assimilation in the basil plant and, consequently, increases yield in this plant.

## Conclusion and outlook

The current study deals with the green-synthesis of nano-fertilizers using leaf extract of the Paulownia trees. Different spectroscopic and microscopic techniques confirmed the synthesized NPs. As mentioned above, TEM results showed an average size of 5–8 nm for NFPs, which indicated good results for Paulownia nanoparticles and was consistent with the results of former studies. The results of FTIR appearance indicated the main distinctive peaks of the NFPs in the spectrum. In addition, the nitrogen peaks in the XPS spectra indicate that the prepared carbon dots NFPs are nitrogen-doped. Moreover, there are functional groups, such as COOH or OH groups on the surface of NFPs.

In the present study, drought stress by increasing oxidative stress increased the lipid peroxidation of the membrane and reduced the content of chlorophylls a, b and total, and through disturbance in the cell, organelle activity and decreasing photosynthetic pigments decreased the basil biological yield. Nano-fertilizers increased the synthesis of soluble proteins and increased the content of chlorophyll and carotenoid by supplying a part of the nutrients required by the plant. Increasing the synthesis of soluble proteins acting as osmotic regulators and protectors improved the status of the plant under stress conditions. It reduced the need to increase the amount of proline and soluble carbohydrates in the plant. On the other hand, increasing the production of photosynthetic pigments and preventing their degradation improved photosynthesis and assimilation, which led to increased plant growth and yield. Therefore, the spraying of the plant by this NFPs could modify some of the effects of drought stress. It is concluded that this green-synthesis NFPs is an easy, cheap, ecofriendly, and bio-stimulating mediator for agriculture purposes. The use of these NFPs for other plants can be effective in modifying the effects of drought stress and improving the yield of these plants, which requires further research in this regard.

**Abbreviations**

NFs: Nanofertilizers; NPs: Nanoparticles; NFP: Nano-fertilizers prepared from Paulownia; IRF: Irrigation levels; PLN: Proline; SP: Soluble proteins; SCA: Soluble carbohydrates; SCW: Soluble carbohydrates in water; Chl a: Chlorophyll a; Chl b: Chlorophyll b; Chl t: Total chlorophyll; CTD: Carotenoid; MDL: Malondialdehyde; BY: Biological yield.

**Acknowledgements**

Not applicable.

**Author contributions**

Conceptualization, YS, and MY; methodology, YS, MY, FSK, KMO, and MH; formal analysis, MCH, YS, MY, FSK, KMO and MH; investigation, YS, MY, and FSK.; resources, MI; data curation, YS, FSK, MH, and ARY; writing—original draft preparation, YS, MH, ARY, and MI; writing—review and editing, YS, ARY, AM and MI; supervision, MI. All authors have read and agreed to the published version of the manuscript.

**Funding**

The authors declare that no funds, grants, or other support were received during the preparation of this manuscript.

**Availability of data and materials**

Are available on request.

## Declarations

**Ethics approval and consent to participate**

All authors whose names appear on the submission have participated.

**Consent for publication**

All authors whose names appear on the submission agree to be published.

**Competing interests**

The authors have no relevant financial or non-financial interests to disclose.

**Author details**

[1]Department of Agronomy and Plant Breeding, University of Kurdistan, Sanandaj, Iran. [2]Department of Plant Production & Genetics, University of Zanjan, Zanjan 4537138791, Iran. [3]Department of Chemistry, Collage of Science, University of Sulaimani, Qliasan St, 46002 Sulaymaniyah, Kurdistan, Iraq. [4]Komar University of Science and Technology, Sulaymaniyah, Kurdistan Region, Iraq.

Received: 2 August 2022 Accepted: 27 October 2022
Published online: 08 November 2022

**References**

1. Manikandan A, Subramanian K. Evaluation of zeolite based nitrogen nano-fertilizers on maize growth, yield and quality on inceptisols and alfisols. Int J Plant Soil Sci. 2016;9(4):1–9.
2. Guo H, White JC, Wang Z, Xing B. Nano-enabled fertilizers to control the release and use efficiency of nutrients. Curr Opin Environ Sci Health. 2018;6:77–83.
3. Heydari M, Yousefi AR, Nikfarjam N, Rahdar A, Kyzas GZ, Bilal M. Plant-based nanoparticles prepared from protein containing tribenuron-methyl: fabrication, characterization, and application. Chem Biol Technol Agric. 2021;8(1):1–11.
4. Heydari M, Yousefi AR, Rahdar A, Nikfarjam N, Jamshidi K, Bilal M, et al. Microemulsions of tribenuron-methyl using Pluronic F127: physico-chemical characterization and efficiency on wheat weed. J Mol Liq. 2021;326:115263.
5. Hassanisaadi M, Barani M, Rahdar A, Heidary M, Thysiadou A, Kyzas GZ. Role of agrochemical-based nanomaterials in plants: biotic and abiotic stress with germination improvement of seeds. Plant Growth Regul. 2022. https://doi.org/10.1007/s10725-021-00782-w.
6. Tarafdar J, Raliya R, Rathore I. Microbial synthesis of phosphorous nanoparticle from tri-calcium phosphate using *Aspergillus tubingensis* TFR-5. J Bionanosci. 2012;6(2):84–9.
7. Farrell J, Kason M, Melitas N, Li T. Investigation of the long-term performance of zero-valent iron for reductive dechlorination of trichloroethylene. Environ Sci Technol. 2000;34(3):514–21.
8. Heydari M, Mir N, Moussavi-Nik SM. Reducing nitrogen loss by application of natural clinoptilolite modified with quaternary N-Alkyl agent as controlled-release fertilizer in two species of beans (*P. vulgaris* and *Vigna Unguiculata*). Commun Soil Sci Plant Anal. 2018;49(13):1586–603.
9. Chandra H, Patel D, Kumari P, Jangwan J, Yadav S. Phyto-mediated synthesis of zinc oxide nanoparticles of *Berberis aristata*: characterization, antioxidant activity and antibacterial activity with special reference to urinary tract pathogens. Mater Sci Eng, C. 2019;102:212–20.
10. Khamlich S, Manikandan E, Ngom B, Sithole J, Nemraoui O, Zorkani I, et al. Synthesis, characterization, and growth mechanism of α-Cr2O3 monodispersed particles. J Phys Chem Solids. 2011;72(6):714–8.
11. Ovais M, Khalil AT, Islam NU, Ahmad I, Ayaz M, Saravanan M, et al. Role of plant phytochemicals and microbial enzymes in biosynthesis of metallic nanoparticles. Appl Microbiol Biotechnol. 2018;102(16):6799–814.
12. Iqbal J, Abbasi BA, Ahmad R, Mahmoodi M, Munir A, Zahra SA, et al. Phytogenic synthesis of nickel oxide nanoparticles (NiO) using fresh leaves extract of *Rhamnus triquetra* (wall.) and investigation of its multiple in vitro biological potentials. Biomedicines. 2020;8(5):117.
13. Iqbal J, Abbasi BA, Ahmad R, Mahmood T, Ali B, Khalil AT, et al. Nanomedicines for developing cancer nanotherapeutics: from benchtop to bedside and beyond. Appl Microbiol Biotechnol. 2018;102(22):9449–70.
14. Khalil AT, Ovais M, Ullah I, Ali M, Shinwari ZK, Hassan D, et al. Sageretia thea (Osbeck) modulated biosynthesis of NiO nanoparticles and their in vitro pharmacognostic, antioxidant and cytotoxic potential. Artif cells Nanomed Biotechnol. 2018;46(4):838–52.
15. Iqbal J, Abbasi BA, Batool R, Mahmood T, Ali B, Khalil AT, et al. Potential phytocompounds for developing breast cancer therapeutics: nature's healing touch. Eur J Pharmacol. 2018;827:125–48.
16. Zhu Z, Chao C, Lu X, Xiong Y. Paulownia in China: cultivation and utilization. Beijing: Asian Network for Biological Science and International Development Research Centre, Chinese Academy of Forestry; 1986.
17. Caparrós S, Díaz M, Ariza J, López F, Jiménez L. New perspectives for *Paulownia fortunei L.* valorisation of the autohydrolysis and pulping processes. Bioresour Technol. 2008;99(4):741–9.
18. Bergmann BA. Propagation method influences first year field survival and growth of Paulownia. New For. 1998;16(3):251–64.
19. Silvestre AJ, Evtuguin DV, Sousa APM, Silva AM. Lignans from a hybrid Paulownia wood. Biochem Syst Ecol. 2005;12(33):1298–302.

20. Liao L, Mei H, Li J, Li Z. Estimation and prediction on retention times of components from essential oil of Paulownia tomentosa flowers by molecular electronegativity-distance vector (MEDV). J Mol Struct (Thoechem). 2008;850(1–3):1–8.
21. Vlase L, Benedec D, Hanganu D, Damian G, Csillag I, Sevastre B, et al. Evaluation of antioxidant and antimicrobial activities and phenolic profile for Hyssopus officinalis *Ocimum basilicum* and *Teucrium chamaedrys*. Molecules. 2014;19(5):5490–507.
22. Damalas CA. Improving drought tolerance in sweet basil (*Ocimum basilicum*) with salicylic acid. Sci Hortic. 2019;246:360–5.
23. Kumar P, Kumar M, Kavitha K, Singh J, Khan R. Pharmacological actions of *Ocimum sanctum*–review article. Int J Adv Pharm, Biol Chem. 2012;1(3):2277–4688.
24. Nadeem M, Abbasi BH, Younas M, Ahmad W, Zahir A, Hano C. LED-enhanced biosynthesis of biologically active ingredients in callus cultures of *Ocimum basilicum*. J Photochem Photobiol, B. 2019;190:172–8.
25. Chiang LC, Ng LT, Cheng PW, Chiang W, Lin CC. Antiviral activities of extracts and selected pure constituents of *Ocimum basilicum*. Clin Exp Pharmacol Physiol. 2005;32(10):811–6.
26. Nakabayashi R, Saito K. Integrated metabolomics for abiotic stress responses in plants. Curr Opin Plant Biol. 2015;24:10–6.
27. Kumar SN. Improving crop adaptations to climate change: contextualizing the strategy. In: Minhas PS, Rane J, Pasala RK, editors. Abiotic stress management for resilient agriculture. Singapore: Springer; 2017. p. 277–98.
28. Barchet GL, Dauwe R, Guy RD, Schroeder WR, Soolanayakanahally RY, Campbell MM, et al. Investigating the drought-stress response of hybrid poplar genotypes by metabolite profiling. Tree Physiol. 2014;34(11):1203–19.
29. Sanchez DH, Schwabe F, Erban A, Udvardi MK, Kopka J. Comparative metabolomics of drought acclimation in model and forage legumes. Plant, Cell Environ. 2012;35(1):136–49.
30. Ashrafi M, Azimi-Moqadam M-R, Moradi P, MohseniFard E, Shekari F, Kompany-Zareh M. Effect of drought stress on metabolite adjustments in drought tolerant and sensitive thyme. Plant Physiol Biochem. 2018;132:391–9.
31. Bates LS, Waldren RP, Teare I. Rapid determination of free proline for water-stress studies. Plant Soil. 1973;39(1):205–7.
32. Bradford MM. A rapid and sensitive method for the quantitation of microgram quantities of protein utilizing the principle of protein-dye binding. Anal Biochem. 1976;72(1–2):248–54.
33. Yemm E, Willis A. The estimation of carbohydrates in plant extracts by anthrone. Biochemical journal. 1954;57(3):508.
34. Lichtenthaler HK, Buschmann C. Chlorophylls and carotenoids: measurement and characterization by UV-VIS spectroscopy. Curr Protoc Food Anal Chem. 2001. https://doi.org/10.1002/0471142913.faf0403s01.
35. Heath RL, Packer L. Photoperoxidation in isolated chloroplasts: I. kinetics and stoichiometry of fatty acid peroxidation. Arch Biochem Biophys. 1968;125(1):189–98.
36. Omer KM, Hassan AQ. Chelation-enhanced fluorescence of phosphorus doped carbon nanodots for multi-ion detection. Microchim Acta. 2017;184(7):2063–71.
37. Omer KM, Tofiq DI, Hassan AQ. Solvothermal synthesis of phosphorus and nitrogen doped carbon quantum dots as a fluorescent probe for iron (III). Microchim Acta. 2018;185(10):1–8.
38. Omer KM, Aziz KHH, Salih YM, Tofiq DI, Hassan AQ. Photoluminescence enhancement via microwave irradiation of carbon quantum dots derived from solvothermal synthesis of l-arginine. New J Chem. 2019;43(2):689–95.
39. Liu D, Qu F, Zhao X, You J. Generalized one-pot strategy enabling different surface functionalizations of carbon nanodots to produce dual emissions in alcohol–water binary systems. J Phys Chem C. 2015;119(31):17979–87.
40. Bao L, Zhang ZL, Tian ZQ, Zhang L, Liu C, Lin Y, et al. Electrochemical tuning of luminescent carbon nanodots: from preparation to luminescence mechanism. Adv Mater. 2011;23(48):5801–6.
41. Ding H, Du F, Liu P, Chen Z, Shen J. DNA–carbon dots function as fluorescent vehicles for drug delivery. ACS Appl Mater Interfaces. 2015;7(12):6889–97.
42. Sharma P, Jha AB, Dubey RS, Pessarakli M. Reactive oxygen species, oxidative damage, and antioxidative defense mechanism in plants under stressful conditions. J Bot. 2012. https://doi.org/10.1155/2012/217037.
43. Miller G, Suzuki N, Ciftci-Yilmaz S, Mittler R. Reactive oxygen species homeostasis and signalling during drought and salinity stresses. Plant, Cell Environ. 2010;33(4):453–67.
44. Hasanuzzaman M, Nahar K, Fujita M. Extreme temperature responses, oxidative stress and antioxidant defense in plants. Abiotic stress-plant responses Appl Agric. 2013;13:169–205.
45. Lokhande VH, Nikam TD, Penna S. Biochemical, physiological and growth changes in response to salinity in callus cultures of *Sesuvium portulacastrum L*. Plant Cell, Tissue Organ C. 2010;102(1):17–25.
46. Ullah N, Yüce M, Neslihan Öztürk Gökçe Z, Budak H. Comparative metabolite profiling of drought stress in roots and leaves of seven Triticeae species. BMC Genomics. 2017;18(1):1–12.
47. Zhang J, Chen G, Zhao P, Zhou Q, Zhao X. The abundance of certain metabolites responds to drought stress in the highly drought tolerant plant *Caragana korshinskii*. Acta Physiol Plant. 2017;39(5):1–11.
48. Seki M, Umezawa T, Urano K, Shinozaki K. Regulatory metabolic networks in drought stress responses. Curr Opin Plant Biol. 2007;10(3):296–302.
49. Hatami M, Kariman K, Ghorbanpour M. Engineered nanomaterial-mediated changes in the metabolism of terrestrial plants. Sci Total Environ. 2016;571:275–91.
50. Slama I, Ghnaya T, Hessini K, Messedi D, Savouré A, Abdelly C. Comparative study of the effects of mannitol and PEG osmotic stress on growth and solute accumulation in Sesuvium portulacastrum. Environ Exp Bot. 2007;61(1):10–7.
51. Hassanpour H, Khavari-Nejad RA, Niknam V, Najafi F, Razavi K. Penconazole induced changes in photosynthesis, ion acquisition and protein profile of Mentha pulegium L. under drought stress. Physiol Mol Biol Plants. 2013;19(4):489–98.
52. Zandalinas SI, Mittler R, Balfagón D, Arbona V, Gómez-Cadenas A. Plant adaptations to the combination of drought and high temperatures. Physiol Plant. 2018;162(1):2–12.
53. Türkan I, Bor M, Özdemir F, Koca H. Differential responses of lipid peroxidation and antioxidants in the leaves of drought-tolerant P. acutifolius Gray and drought-sensitive P. vulgaris L. subjected to polyethylene glycol mediated water stress. Plant Sci. 2005;168(1):223–31.
54. Bistgani ZE, Siadat SA, Bakhshandeh A, Pirbalouti AG, Hashemi M. Interactive effects of drought stress and chitosan application on physiological characteristics and essential oil yield of Thymus daenensis Celak. Crop J. 2017;5(5):407–15.
55. Mohasseli V, Sadeghi S. Exogenously applied sodium nitroprusside improves physiological attributes and essential oil yield of two drought susceptible and resistant specie of Thymus under reduced irrigation. Ind Crops Prod. 2019;130:130–6.
56. Oukarroum A, Schansker G, Strasser RJ. Drought stress effects on photosystem I content and photosystem II thermotolerance analyzed using Chl a fluorescence kinetics in barley varieties differing in their drought tolerance. Physiol Plant. 2009;137(2):188–99.
57. Kausar R, Arshad M, Shahzad A, Komatsu S. Proteomics analysis of sensitive and tolerant barley genotypes under drought stress. Amino Acids. 2013;44(2):345–59.
58. Hatami M, Ghorbanpour M. Defense enzyme activities and biochemical variations of Pelargonium zonale in response to nanosilver application and dark storage. Turk J Biol. 2014;38(1):130–9.
59. Hossain Z, Yasmeen F, Komatsu S. Nanoparticles: synthesis, morphophysiological effects, and proteomic responses of crop plants. Int J Mol Sci. 2020;21(9):3056.
60. Ghorbanpour M, Hatami M. Changes in growth, antioxidant defense system and major essential oils constituents of Pelargonium graveolens plant exposed to nano-scale silver and thidiazuron. Indian J Plant Physiol. 2015;20(2):116–23.
61. Aghdam MTB, Mohammadi H, Ghorbanpour M. Effects of nanoparticulate anatase titanium dioxide on physiological and biochemical performance of Linum usitatissimum (Linaceae) under well-watered and drought stress conditions. Brazilian J Botany. 2016;39(1):139–46.
62. Liu R, Lal R. Synthetic apatite nanoparticles as a phosphorus fertilizer for soybean (Glycine max). Sci Rep. 2014;4(1):1–6.


## Publisher's Note